Research Article

Journal of Environmental Nanotechnology

Novel Design of a Pilot-scale Bioethanol Production Plant Using Municipal Organic Waste

Neha Verma Gour[1], Preeti Singh[1*], Nishant Dwivedi[1] and R. N. Singh[2]

[1]Department of Electrical Engineering, Medicaps University, Indore, MP, India
[2]School of Energy and Environmental Studies, DAVV, Indore

Received: 10.02.2026 Accepted: 25.03.2026 Published: 30.03.2026

*preeti.singh.ee@medicaps.a.c.in

ABSTRACT

The increasing demand for renewable fuels has accelerated interest in converting municipal organic waste (MOW) into bioethanol. This study presents the complete design, engineering development, and performance assessment of a pilot-scale bioethanol production reactor capable of processing 5 tons of wet MOW per batch. The system integrates pre-treatment, drying, hydrolysis, fermentation, and distillation units within a semi-automated configuration. Each subsystem of the pilot-level continuous bioethanol production system was designed based on experimental results and engineering calculations. The process successfully demonstrates the technical feasibility of scaling laboratory experiments to a pilot-level continuous bioethanol production system. The results confirm the potential of urban organic waste as a sustainable feedstock for clean fuel generation, thereby maximizing conversion efficiency and supporting circular bioeconomy and waste valorization strategies.

Keywords: Bioethanol production; Municipal organic waste; Pilot-scale reactor; Hydrolysis; Fermentation; Distillation; Waste-to-energy.

1. INTRODUCTION

The increasing global demand for renewable, environmentally sustainable energy sources has intensified research into bioethanol production from low-cost, abundant biomass. Municipal Organic Waste (MOW), which constitutes a significant fraction of solid waste generated in urban areas, presents a promising feedstock for second-generation bioethanol. Its high carbohydrate content and continuous availability make it an attractive alternative to traditional agricultural biomass, while simultaneously addressing waste management challenges and reducing landfill burdens (Biose *et al.* 2021). Pilot-scale technologies play a critical role in bridging the gap between laboratory experiments and industrial bioethanol production, as shown in Fig. 1.

They provide a realistic framework for validating process parameters, optimizing reaction conditions, and assessing engineering feasibility before large-scale deployment. Recent advances in bioethanol reactor design emphasize integrated systems that combine pre-treatment, hydrolysis, fermentation, and distillation within a compact and energy-efficient configuration. The present study focuses on the design and development of a fully integrated pilot-scale bioethanol production reactor capable of processing 5 tons of wet MOW per batch. The system incorporates solar and electric drying, mechanical size reduction, acid hydrolysis, pH adjustment and nutrient preparation, fermentation, and ethanol recovery units (Arijana *et al.* 2018). This research aims to establish a scalable engineering model for converting MOW into bioethanol, promoting circular bioeconomy practices. The proposed reactor configuration demonstrates the potential for continuous, cost-effective, and environmentally viable bioethanol production from municipal waste streams (Ravichandran *et al.* 2022).

2. MATERIALS AND METHODS

2.1 Materials

MOW generated within the urban municipal region in Indore, India, was collected through routine waste-handling operations and immediately transferred to the pilot facility, where 5 tonnes of heterogeneous, high-moisture biomass were homogenized in a 27 m^3 reinforced concrete containment unit engineered for mechanical robustness, microbial resistance, and prolonged exposure to corrosive leachates. Before processing, the feedstock underwent compositional assessment to verify suitability for biochemical conversion, with average moisture content quantified at ~78% as shown in Fig. 2. The homogenized stream was metered via a stainless-steel conveyor, where enhanced greenhouse trapping elevated internal temperatures enabling evaporative removal of approximately 3900 kg of water over 24–48 hours. To maintain operational continuity irrespective of climatic variability, an electrically driven 550 kW forced-convection dryer

operating at 60 °C was incorporated to achieve controlled thermal dewatering. The dried biomass (~1100 kg) was subsequently subjected to particle size reduction, yielding a fine particulate substrate (<5 mm) optimized for mass transfer and reagent penetration during pre-treatment. Acid hydrolysis was facilitated through preparation of a 3% w/w H_2SO_4 solution in a 12,000 L FRP chemical-resistant mixing chamber using precision-controlled metering of concentrated acid (335.5 L) into water (10,664.5 L), followed by transfer into a 17.16 m³ SS316L, Teflon-lined, jacketed hydrolysis reactor where a 1:10 solid-to-liquid ratio was maintained. Post-hydrolysis, the liquor was rapidly cooled, filtered to remove recalcitrant solids, and routed to an 11.5 m³ pH-conditioning vessel where 2 N NaOH (705 L) was introduced via automated dosing to achieve a fermentation-compatible pH of 5. Concurrently, a defined nutrient medium comprising glucose, peptone, yeast extract, and urea was formulated in a 10,000 L SS316L fermentation-media bioreactor, while yeast activation was performed in a 6500 L aerated pre-culture reactor under controlled agitation and oxygen transfer to augment biomass concentration and metabolic readiness (Devi *et al.* 2023).

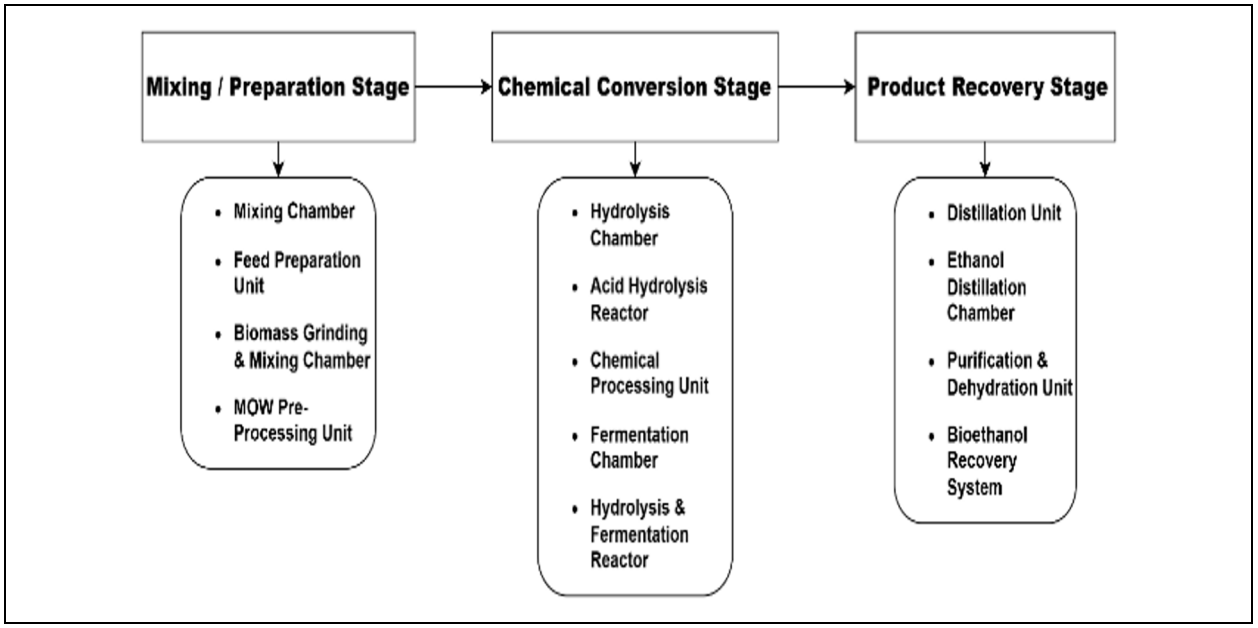


Fig. 1: Block diagram of the integrated bioethanol production system

2.2 Characterization

The neutralized hydrolysate, nutrient medium, and yeast inoculum were subsequently co-fed into a 20,000 L SS316L fermentation reactor, maintaining a 5:3:2 volumetric ratio, where anaerobic fermentation proceeded at 30 °C for 72 hours with regulated agitation and continuous CO_2 disengagement to prevent mass transfer limitations (Zentou *et al.* 2023). Upon completion, the resultant beer was distilled through a 6-m-high packed fractional distillation column (850–900 mm internal diameter), driven by a 300 kW reboiler and coupled with a 20 m³ h^{-1} cooling circuit, enabling recovery of ~95% purity bioethanol. Final dehydration using sodium sulphate ensured minimal residual water content. The purified bioethanol was stored in a 30 m³ epoxy-lined carbon steel tank outfitted with a floating roof, pressure-vacuum safety controls, grounding provisions, and emission-minimizing features. Throughout the workflow, all critical operational parameters were continuously logged and monitored to ensure reproducibility, regulatory compliance, and fidelity of process performance (Yan *et al.* 2024). Table 1 presents an overall summary of the system, highlighting its key components, operational features, and performance characteristics.

Table 1. Overall system summary

Stage	Input	Output
Waste Storage	Raw waste	Stored waste
Solar Drying	Stored waste	Partially dried waste
Electric Drying	Partially dried waste	Fully dried waste
Grinding and Mixing	Dried waste	Uniform powder
Acid Hydrolysis	Powder + acid + heat	Hydrolyzed slurry
pH Adjustment	Acidic slurry + base	Neutralized slurry
Fermentation	Neutralized slurry + yeast	Fermented broth
Distillation	Fermented broth	Ethanol + stillage
Ethanol Storage	Purified ethanol	Stored bioethanol

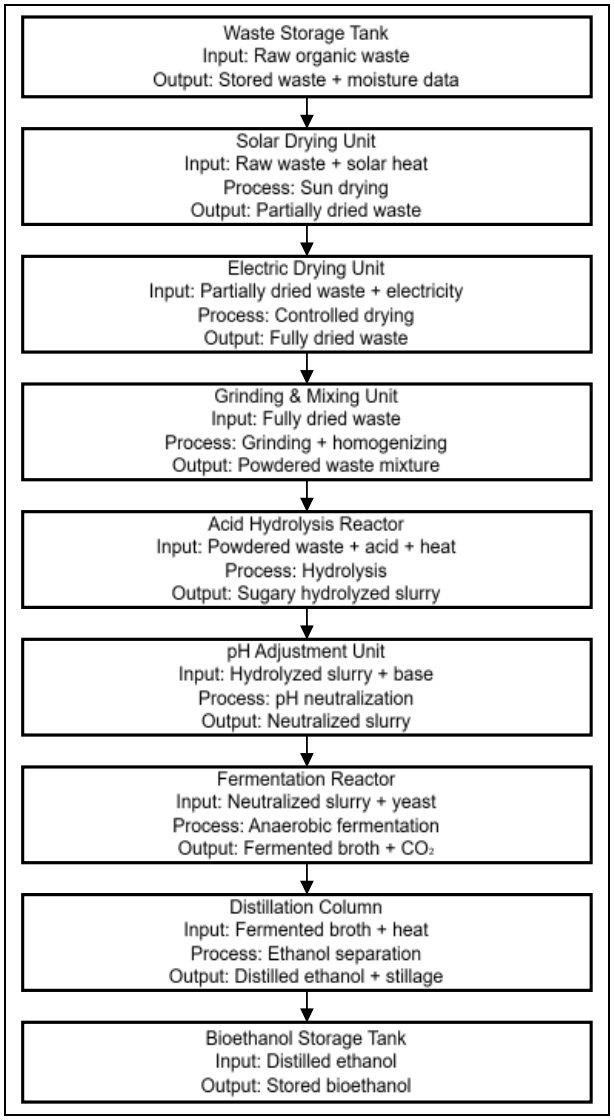


Fig. 2: Flowchart for bioethanol production from organic waste

3. DESIGN OF REACTOR COMPONENTS

The pilot-scale bioethanol production system was engineered as an integrated sequence of interconnected unit operations designed to process 5 tonnes of wet MOW per batch. Each component was dimensioned through detailed mass–energy balances, material-property evaluations, and process optimization constraints to ensure stable operation, efficient conversion, and scalability toward industrial implementation (Khan *et al.* 2023).

3.1 Design of Reactor Components

The feedstock storage tank was designed as a 27 m^3 reinforced concrete structure to accommodate the volumetric expansion associated with gaseous by-products and heterogeneous waste composition shown in Fig. 3. A 3 × 3 × 3 m geometry was selected to enable efficient dumping from municipal vehicles, minimize dead zones and support continuous feeding through a mechanical conveyor while resisting microbial degradation and moisture-induced deterioration. It was found that for 170 kg of the as-received MOW occupies a volume of 0.8 m^3, so the volume required for 5 tons of the as-received MOW is:

$$\frac{0.8\ m^3 \times 5000\ kg}{170\ kg} = 23.52\ m^3 \quad \ldots (1)$$

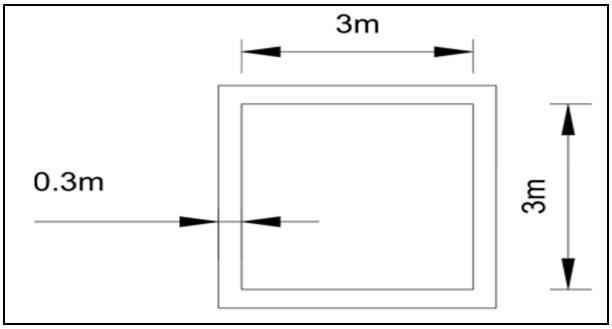


Fig. 3: Cross-sectional view of feedstock storage tank

A 10 m stainless-steel conveyor system (SS304) was incorporated to facilitate controlled and hygienic transfer of MOW to the drying units (Broda *et al.* 2022).

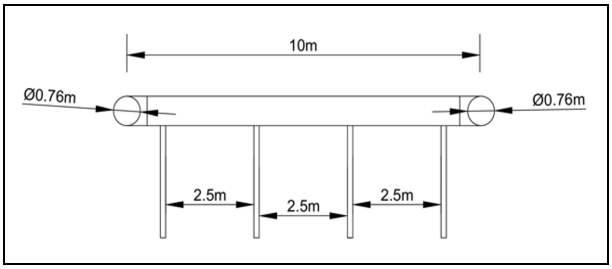


Fig. 4: Designed conveyor

Table 2: Performance estimation of the designed solar dryer

Parameter	Value
Initial moisture content	78%
Total water to be removed	3,900 kg
Total energy required for drying	≈ 8.81 × 10^6 kJ
Estimated drying duration	~2 days (under sunny conditions)
Required solar collector area	900 m^2
Dryer type	Direct sun-drying solar greenhouse dryer
Expected internal temperature	40–60 °C (during peak sunlight)

Design considerations, as shown in Fig. 4, included belt width (400 mm), corrosion resistance, minimal friction losses, and a 0.5 HP geared motor capable of maintaining 10–20 m min^{-1} transport velocity, optimized for intermittent start–stop operation (Barbir *et al.* 1990)

Moisture reduction, a critical determinant of hydrolysis efficiency, was achieved via two parallel drying systems. Table 2 presents the performance estimations of the designed solar dryer under the specified operating conditions.

Complementarily, a 550-kW electrical hot-air dryer was engineered using convective heat transfer modeling to maintain a uniform 60 °C drying temperature (Beluhan *et al.* 2023), ensuring year-round operability and process continuity.

As an alternative to the solar dryer, an electric dryer has been installed in parallel for emergency use, such as during the rainy season. The dryer is designed to dry 5 tons of as-received MOW (Kazmi *et al.* 2025). The dryer is designed for the wet MOW, considering it will have a maximum moisture content of 78%. Initially, the drying time is 8 hours/day, which can be adjusted as per need. This drying time is suitable for the proper functioning and maintenance of the dryer. To avoid burning of the MOW, the drying temperature is kept at 60 °C. The average ambient temperature is considered to be 25–30 °C. The electric dryer works on the methods of electrical heating and convective hot air flow. The final heater rating can be designed as 550 kW. The dryer is a batch-type electric hot air dryer. It uses electric heaters and a blower fan to circulate hot air (Al-Hammadi *et al.* 2025).

To grind and homogenize 1100 kg of the dry MOW per batch, a grinding and mixing chamber is designed (Palaniappan *et al.* 2025). The bulk density of the MOW is approximately 250–300 kg/m³. The system incorporates either a hammer mill or cutter blades within the chamber, powered by a 5–7.5 HP motor suitable for processing fibrous dry matter, with blade speeds ranging from 1000 to 1500 rpm and replaceable screens for achieving particle sizes below 5 mm (Shukla *et al.* 2024). The construction materials include an SS304 body for corrosion resistance, hardened steel or stainless-steel blades and shaft, and sealed, dust-proof bearings to ensure durability and reliable performance (Chamoli *et al.* 2024).

For hydrolysis, the required ratio of the dry MOW and acid solution is 1:10. The weight of the dry MOW is 1,100 kg, so the required quantity of the acid solution is 11,000 L. The purity of the acid is assumed to be 98%. In the experimental research, it was found that for 100 mL of the required acid solution, 3.05 mL of acid and the remaining 96.95 mL of water are required. The chamber is designed with a total capacity of 12,000 L, providing a 10% buffer above the 11,000-litre operating volume to prevent overflow and ensure adequate mixing space (Siddique *et al.* 2024).

3.2 Design of Hydrolysis Chamber

The hydrolysis input process parameters are presented in Table 3. This is a batch-type closed lid reactor in which a heated jacket or steam-heated vessel has been used. It is made of 316 L with a Teflon-coated interior for acid resistance and durability. For heating the chamber, a solar-heated water bath is preferred. An electric heating jacket is also provided as an option. A magnetic stirrer is used in laboratory-scale reactors for effective mixing of the chemicals, whereas a motor-driven impeller can be installed in larger units.

Table 3. Hydrolysis input process parameters

Parameter	Value
Dry organic waste	1100 kg
Acid solution volume	11000 L
Acid concentration	3% H_2SO_4 (w/w)
Solid to liquid ratio (S:L)	1:10
Reaction temperature	100–130 °C
Reaction time	20–30 minutes
Pressure (if sealed)	1 bar (optional for fast hydrolysis)

A headspace margin was provided in the reactor to ensure proper mixing and boiling of the liquid. The weight of the dry MOW is 1100 kg. The density of the dry ground MOW is assumed to be 500 kg/m^3.

A motor of 2 HP is required for mixing 3 m³ of slurry. It is recommended to wear PPE as 3% H_2SO_4 is mildly corrosive, use acid-resistant tubing and seals (Viton or PTFE), and include a vent or pressure relief valve.

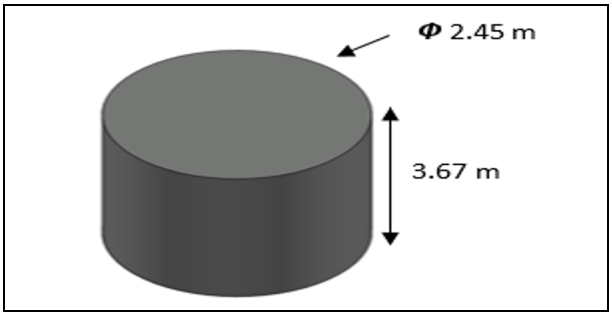


Fig. 5: Outer shape of hydrolysis chamber

To ensure safe operation and mixing, 30% extra volume (freeboard) is considered, so the design volume becomes 8,812 x 1.3 = 11,455.6 L. After rounding up, the design volume is 11,500 L. The tank is designed as a cylindrical vessel (Fig. 5) following a height-to-diameter ratio of 1.5, which is commonly adopted for efficient mixing performance (Rajeswari *et al.* 2022). This configuration provides a balanced design that supports uniform flow patterns and stable mixing conditions. The fermentation media chamber is designed to prepare a nutrient-rich fermentation medium that supports

microbial growth and ethanol production during fermentation. In the production of bioethanol from MOW, this chamber enables controlled mixing of glucose, peptone, yeast extract, and urea with water (Nair *et al.* 2020). The mixture helps to maintain optimal pH and nutrient balance before being supplied to the fermentation vessel through stainless steel pipelines.

Table 4. Design specifications of chambers

Fermentation Media Chamber		Yeast Suspension Chamber	
Parameter	**Specification**	**Parameter**	**Specification**
Capacity	8000 L (80% working capacity of 10,000 L vessel)	Capacity	5000 L (75% working volume of 6500 L vessel)
Material of construction	Stainless Steel 316L, internally polished	Material of construction	Stainless Steel 316L
Shape	Cylindrical, vertical orientation	Shape	Cylindrical, vertical orientation
Headspace allocation	20% of total volume	Height-to-diameter ratio (H:D ratio)	0.084027778
H:D	0.084027778	Agitation	3–5 kW motor with Rushton turbine
Pressure	Atmospheric (1 atm)	Duration of operation	24-hour batch cycle

The yeast suspension chamber allows yeast culture activation and growth before fermentation. In this chamber, yeast is maintained under controlled environmental and nutritional conditions, usually with added glucose (20 g/L), yeast extract (10 g/L), and ammonium sulfate (1 g/L) for a 24-hour growth period (Coşgun *et al.* 2023). Table 4 outlines the design specifications of the fermentation media and yeast suspension chambers.

4. RESULTS AND DISCUSSION

The integrated pilot-scale system demonstrated effective conversion of MOW into fuel-grade ethanol. Drying performance was efficient, reducing initial moisture from 78% to 22%, approximately. Solar drying removed around 3900 kg of water per batch, while the auxiliary electric dryer ensured uniformity and continuity during low-irradiance periods (David *et al.* 2023). The hybrid configuration reduced drying variability and established stable conditions for downstream processing.

Feed Mass:

$$\text{mass} = \rho_{mix} \times \text{volume}$$

$$= 0.88204 \times 1000.0$$

$$= 882.04 \text{ kg}$$

Ethanol Mass in Feed:

$$eth_{mass} = \text{mass} \times 0.4963$$

$$= 882.04 \times 0.4963$$

$$= 437.75 \text{ kg}$$

Total Distillate Mass Required (Dtotal) to Collect that Ethanol at 95 wt.%:

$$D_{total} = eth_{mass} \div 0.95$$

$$= 437.75 \div 0.95$$

$$= 460.79 \approx 460.79 \text{ kg}$$

Average Distillate Mass Flow ($\dot{D}$) Over 1.5 h:

$$\dot{D} = D_{total} \div 1.5$$

$$= 460.79 \div 1.5$$

$$= 307.19 \text{ kg/h}$$

A reflux ratio (R) of 2 is assumed.

Overhead (vapor) Mass Flow (Using $\dot{V} = \dot{D} \times (R + 1)$):

$$\dot{V} = 307.19 \times 3.0$$

$$= 921.59 \text{ kg/h}$$

Hourly Latent Energy Q_kJ/h ≈ $\dot{V}$ × 900 kJ/kg:

$$Q_kJ/h = 921.59 \times 900$$

$$= 829{,}434.59 \text{kJ/h}$$

Converting to kW (kJ/s) by Dividing by 3600:

$$Q_kW = 829{,}434.59 \div 3600$$

$$= 230.39 \text{ kW}$$

Cooling Water for Condenser:

$Cp_{water} \approx 4.18$ kJ/kg·K; $\Delta T = 10$ K:

$$C_w_mass_flow \text{ (kg/s)} = Q_kW \div (C_p \times \Delta T)$$

$$= 230.39 \div (4.18 \times 10)$$

$$= 5.51 \text{ kg/s}$$

Converting to m³/h:

$$5.51 \times 3600 = 19{,}840.25 \text{ kg/h} \approx 19.84 \text{ m}^3\text{/h}$$

Recommend design cooling water flow ≈ 20–22 m³/h (allowing fouling margins).

Column internal sizing, packing height, and diameter were determined based on the high vapor traffic (≈ 922 kg/h), which results in a substantial increase in column diameter. To attain an ethanol concentration of 95 wt.% (approx.) from the initial 49.6 wt.%, approximately 10 to 15 stages are required by using structured packing with a typical height equivalent to a theoretical plate (HETP) of 0.4 to 0.6 m. A packing height of 6 m was designated as a baseline strategy. The column diameter was assessed using practical scaling. Former designs indicate that a DN150 column is capable of handling 39 kg/h of vapor, while a DN400 column can handle about 208 kg/h. For a current system with a vapor flow rate of around 921.6 kg/h, the required diameter is 2.1 times that of the DN400 column. This corresponds to an internal diameter of 0.84 m. Kettle working volume to keep a comfortable headspace for vigorous boil-up is 1.5–2.0 m^3 working volume for a 1000 L charge with a high boil rate. The steam jacket immersion size is around 300 kW duty (≈377 kg/h steam). Agitation provides gentle agitation or recirculation to avoid bumping and ensure uniform heat transfer (Yiin *et al.* 2022). Reflux drum size design for 5–10 minutes of holdup at high distillate rates plus surge capacity recommends approximately 500–1000 L working vessel (750 L is a good compromise). The reflux pump must be capable of delivering a maximum reflux flow rate of R×Ḋ.

$$\text{At } R=2 \text{ and } \dot{D} = 307.20 \text{ kg/h} \approx 0.307 \text{ m}^3\text{/h},$$

$$\text{Maximum reflux flow} = R \times \dot{D} \approx 2 \times 0.307$$

$$= 0.614 \text{ m}^3\text{/h}$$

However, to allow for pump turndown and pressure requirements, a pump rated at 1–2 m^3/h and 20–30 m head with a variable frequency drive (VFD) was selected to ensure good control. The distillate transfer pump is a similar small centrifugal pump.

These volumetric pump numbers are small because the liquid distillate volumetric flow is modest, and mass flows are large because vapor density is low; the reflux volumetric flows remain manageable.

4.1 Pressure Drop and ΔP considerations

With very high vapor traffic, pressure drop across packing can increase; choosing low-ΔP structured packing (metal high-capacity packing) and a larger diameter can keep superficial vapor velocity below flooding limits. The total packed-bed ΔP is expected to be <50–100 mbar at the design load, with final values determined using vendor packing data.

4.2 Mechanical Considerations

The column and associated equipment are constructed with wetted parts made of SS304L, with the option to upgrade to SS316L when handling chlorides or aggressive organic compounds. PTFE gaskets and ethanol-compatible mechanical seals are used to ensure leak-free operation, while the system is insulated with 50–75 mm mineral wool and protective cladding (Nwakego and Enajeme, 2025). Due to the tall packing section, maintenance platforms are installed at approximately 3 m and 6 m heights. For a feed of 1000 L containing 49.63 wt.% ethanol, the ethanol mass amounts to about 437.76 kg, requiring a distillate production of roughly 460.80 kg at 95 wt.% purity, corresponding to a throughput of around 307.20 kg/h over a 1.5-hour run. The vapor traffic through the column is about 921.6 kg/h, and the reboiler and condenser must handle a thermal duty of about 230.4 kW; therefore, a 300-kW unit is recommended. Steam consumption is estimated at 377 kg/h at 3–4 bar (g), with cooling water requirements of approximately 20 m^3/h for a 10 °C temperature rise (Faria *et al.* 2024). The distillation column requires a packing height of about 6 m with a shell diameter of 850–900 mm, or the system can be divided into multiple parallel DN500–DN600 columns. The kettle reboiler should have a working capacity of 1.5–2.0 m^3, and the reflux drum is recommended to be approximately 750 L, as illustrated in Fig. 6.

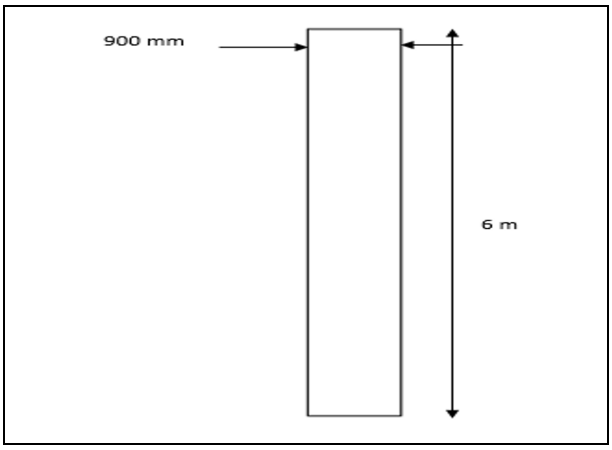


Fig. 6: Column shell

4.3 Design of Bioethanol Storage Tank

Vertical cylindrical tank is made of carbon steel with epoxy internal lining for ethanol compatibility and is equipped with an internal floating roof (IFR) to minimize vapor losses. The storage tank is designed with a total volume of 30 m^3, corresponding to an estimated diameter of approximately 3 m and a height of about 4.3 m, adjustable based on site layout and space availability. The storage tank is constructed with a carbon-steel shell and roof, protected internally with an epoxy or phenolic coating suitable for ethanol service. An aluminum or stainless-steel floating roof equipped with perimeter seals minimizes vapor losses and enhances safety. Key accessories include one or two manways for inspection and maintenance, along with inlet, outlet, overflow, vent, and sampling nozzles (Bhattacharyya *et al.* 2025).

4.4 Proposed Design of Bioethanol Pilot-scale Reactor

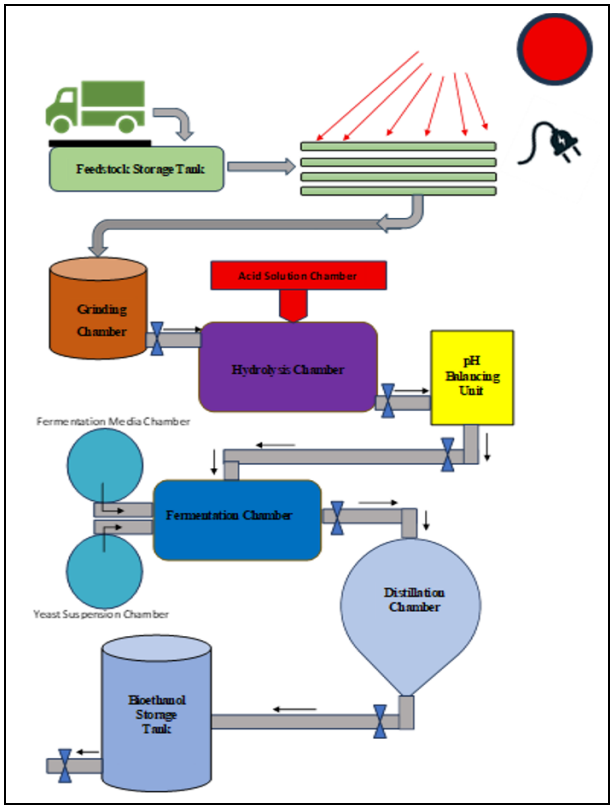


Fig. 7: Designed pilot-scale bioethanol production reactor

Fig. 7 represents the designed pilot-scale bioethanol production reactor. Instrumentation consists of a radar or ultrasonic level sensor, a high-level alarm, and a temperature sensor to ensure proper monitoring. Safety features include a flame arrestor on the vent, grounding and bonding provisions, and a surrounding bund wall with 110% of the tank's volume capacity for spill containment. The foundation comprises a reinforced concrete pad with anchor bolts, situated within the bonded area to safely contain any potential leakage.

5. CONCLUSION

The design and development of a pilot-scale reactor for bioethanol production represents a crucial step toward optimizing sustainable biofuel generation technologies. The studies reviewed and experimental outcomes demonstrate that an effective pilot-scale system depends on multiple integrated aspects of process engineering, including biomass pretreatment, fermentation dynamics, bioreactor configuration, and energy recovery. A small land area is sufficient for the installation of a pilot-scale reactor for the continuous production of bioethanol. The pilot-scale reactor successfully demonstrated the scalability of laboratory bioethanol processes, with design parameters such as reactor volume, agitation speed, and temperature control optimized for efficient fermentation. Experimental results set the stable fermentation parameters with competitive ethanol yields and conversion efficiencies relative to reported pilot-scale systems. Economic and environmental assessments revealed that the system reduces carbon emissions while promoting circular bioeconomy practices through waste valorization. The project provides a scalable and adaptable framework for future industrial bioethanol plants, emphasizing continuous process monitoring, automation, and feedstock diversification.

REFERENCES

Al-Hammadi, M., Anadol, G., Jose, F. M. G., Garcia, J. M., Keskin, T. G. and Mine, G., Scaling bioethanol for the future: the commercialization potential of extremophiles and non-conventional microorganisms, *Front. Energy Res.*, 13, (2025). https://doi.org/10.3389/fenrg.2025.1565273

Arijana, B., Nenad, M., Kundas, S., Galina, M., Halina, B., Mirela, I. S., Komes, D., Novak, S. and Bozidar, S., Bioethanol production from renewable raw materials and its separation and purification: a review, *Food Technol. Biotechnol.*, 56(3), 289–311 (2018). https://doi.org/10.17113/ftb.56.03.18.5546

Barbir, F., Veziroğlu, T. N. and Plass, J. H. J., Environmental damage due to fossil fuel use, *Int. J. Hydrogen Energy*, 15(10), 739–749 (1990). https://doi.org/10.1016/0360-3199(90)90005-J

Beluhan, S., Mihajlovski, K., Šantek, B. and Šantek, I. M., The production of bioethanol from lignocellulosic biomass: Pretreatment methods, fermentation and downstream processing, *Energies,* 16(19), 7003 (2023). https://doi.org/10.3390/en16197003

Bhattacharyya, S. and Pathy, M. P., From blossoms to biofuel: a novel approach to bioethanol production, *Discover Appl. Sci.*, 7, 999(2025). https://doi.org/10.1007/s42452-025-07508-x

Biose, O., Jonah, D. A., Maureen, I., Akenzua, O., Atsegha, B., Okorie, C., James, O. and Dennis, I. I., Design, fabrication and performance test of a pilot scale bioethanol plant with fractional distillation unit, *Am. J. Environ. Sci. Eng.*, 5(4), 4, 124–129(2021). https://doi.org/10.11648/j.ajese.20210504.16

Broda, M., Yelle, J. D. and Serwańska, K., Bioethanol production from lignocellulosic biomass—Challenges and solutions, *Mol.*, 27(24), 8717 (2022). https://doi.org/10.3390/molecules27248717

Bušić, A., Nenad, M., Semjon, K., Galina, M., Halina, B., Mirela, I. S., Komes, D., Novak, S. and Bozidar, S., Bioethanol production from renewable raw materials and its industrial design implications, *Renew. Sustain. Energy Rev.*, 173, 112–125 (2025). https://doi.org/10.17113/ftb.56.03.18.5546

Chamoli, P., Jhildiyal, S., Agrawal, P., Kumar, N. and Singh, P., Recent advances in the processing of Napier grass (Pennisetum purpureum Schumach) as a potential bioenergy crop for bioethanol production, *J. Appl. Bio. Biotechnol.*, 12(4), 144–157 (2024). https://doi.org/10.7324/JABB.2024.154513

Coşgun, A., Günay, M. E. and Yıldırım, R., A critical review of machine learning for lignocellulosic ethanol production via fermentation route, *Biofuel Res. J.*, 10(2), 1859–1875 (2023). https://doi.org/10.18331/brj2023.10.2.5

David, A. J., Abinandan, S., Vaidyanathan, V. K., Xu C. C. and Krishnamurthi, T., A critical review on current status and environmental sustainability of pre-treatment methods for bioethanol production from lignocellulose feedstocks, *3 Biotech*, 13 (7), 233 (2023). https://doi.org/10.1007/s13205-023-03657-1

Devi, A., Bajar, S., Sihag, P., Sheikh, Z. U. D., Singh, A., Kaur, J., Bishnoi, N. R. and Pant, D., A panoramic view of technological landscape for bioethanol production from various generations of feedstocks, *Bioeng.*, 14(1), 81–112 (2023). https://doi.org/10.1080/21655979.2022.2095702

Faria, D. J., Carvalho, A. P. A. D. and Conte-Junior, C. A., Fermentation of biomass and residues from Brazilian agriculture for 2G bioethanol production, *ACS Omega*, 9(39), 40298–40314 (2024). https://doi.org/10.1021/acsomega.4c06579

Kazmi, A., Sultana, T., Ali, A., Nijabat, A., Li, G. and Hou, H., Innovations in bioethanol production: A comprehensive review of feedstock generations and technology advances, *Energy Strategy Rev.*, 57, 101634 (2025). https://doi.org/10.1016/j.esr.2024.101634

Khan, A., Niazi, M. B. K., Ansar, R., Jahan, Z., Javaid, F., Ahmad, R., Anjum, H., Ibrahim, M., and Bokhari, A., Thermochemical conversion of agricultural waste to hydrogen, methane, and biofuels: A review, *Fuel,* 351, 128947 (2023). https://doi.org/10.1016/j.fuel.2023.128947

Liu, J., Yin, Z., Liu, W., Jiang, H., Lu, H., Xiao, Z. and Fan, S., Pilot plant design and technology performance analysis of pervaporation membrane bioreactor with mechanical vapor compression for bioethanol production, *China J. Chem. Eng.*, 82, 57–66 (2025). https://doi.org/10.1016/j.cjche.2025.02.026

Nair, L. G. and Verma, P., Harnessing carbon potential of lignocellulosic biomass: Advances in pretreatments, applications, and the transformative role of machine learning in biorefineries, *Biores. Bioproce.*, 12(1), 97 (2025). https://doi.org/10.1186/s40643-025-00935-z

Nwakego, A. C. and Enajeme, D. A., Advances in bioethanol production: Innovations in feedstocks, pretreatment, and fermentation technologies, *Int. J. Adv. Eng. Manage.*, 7(8), 743–753 (2025). https://doi.org/10.35629/5252-0708743753

Rajeswari, S., Divya, B., Saravanan, P., Rajasimman, M., Rajamohan, N. and Yasser, V., Production of ethanol from biomass – Recent research, scientometric review and future perspectives, *Fuel,* 317, 123448 (2022). https://doi.org/10.1016/j.fuel.2022.123448

Ravichandran, S. R., Venkatachalam, C. D., Sengottian, M., Sekar, S., Kandasamy, S., Subramanian, K. P. R., Purushothaman, K., Chandrasekaran, A. L. and Narayanan, M., A review on hydrothermal liquefaction of algal biomass on process parameters, purification and applications, *Fuel,* 313, 122679 (2022). https://doi.org/10.1016/j.fuel.2021.122679

Siddique, M., Evaluation and composition of lignin content to enable the production of lignocellulosic biomass pretreatment into sustainable biofuel: A review, *Sigma J. Eng. Nat. Sci.*, 42(1), 306–311(2024). https://doi.org/10.14744/sigma.2024.00024

Shukla, A., Malik, T. and Anand, M., Biphasic approach for bioethanol production: Simultaneous oxalic acid pretreatment, saccharification and co-fermentation, *Int. J. Energy Res.,* 2024(1), 8392361(2024). https://doi.org/10.1155/2024/8392361

Yan, S., Chen, X., Wu, J. and Wang, P., Pilot-scale production of fuel ethanol from concentrated food waste hydrolysates using Saccharomyces cerevisiae H058, *Bioprocess Biosyst. Eng.*, 36, 7, 937–946 (2013). https://doi.org/10.1007/s00449-012-0827-9

Yiin, C. L., Odita, E. B., Lock, S. S. M., Cheah, K. W., Chan, Y. H., Wong, M. K., Chin, B. L. F., Quitain, A. T., Loh, S. K. and Yusup, S., A review on potential of green solvents in hydrothermal liquefaction (HTL) of lignin, *Bioresour. Technol.,* 364, 128075 (2022). https://doi.org/10.1016/j.biortech.2022.128075

Zentou H., Abidin Z. Z., Issa M. A., Yunus R. and Awang Biak D. R., Developing an integrated mathematical model of fermentation–pervaporation system for bioethanol production, *Chem. Eng. J.*, 473, 145229(2023). https://doi.org/10.1016/j.cej.2023.145229